Hindawi
Contrast Media & Molecular Imaging
Volume 2023, Article ID 9809608, 1 page
https://doi.org/10.1155/2023/9809608

Retraction

Retracted: Prediction of Changes in Tumor Regression during Radiotherapy for Nasopharyngeal Carcinoma by Using the Computed Tomography-Based Radiomics

Contrast Media & Molecular Imaging

Received 25 July 2023; Accepted 25 July 2023; Published 26 July 2023

This article has been retracted by Hindawi following an investigation undertaken by the publisher [1]. This investigation has uncovered evidence of one or more of the following indicators of systematic manipulation of the publication process:

(1) Discrepancies in scope
(2) Discrepancies in the description of the research reported
(3) Discrepancies between the availability of data and the research described
(4) Inappropriate citations
(5) Incoherent, meaningless and/or irrelevant content included in the article
(6) Peer-review manipulation

The presence of these indicators undermines our confidence in the integrity of the article's content and we cannot, therefore, vouch for its reliability. Please note that this notice is intended solely to alert readers that the content of this article is unreliable. We have not investigated whether authors were aware of or involved in the systematic manipulation of the publication process.

In addition, our investigation has also shown that one or more of the following human-subject reporting requirements has not been met in this article: ethical approval by an Institutional Review Board (IRB) committee or equivalent, patient/participant consent to participate, and/or agreement to publish patient/participant details (where relevant).

Wiley and Hindawi regrets that the usual quality checks did not identify these issues before publication and have since put additional measures in place to safeguard research integrity.

We wish to credit our own Research Integrity and Research Publishing teams and anonymous and named external researchers and research integrity experts for contributing to this investigation.

The corresponding author, as the representative of all authors, has been given the opportunity to register their agreement or disagreement to this retraction. We have kept a record of any response received.

References

[1] Y. Yang, J. Wu, W. Mai, and H. Li, "Prediction of Changes in Tumor Regression during Radiotherapy for Nasopharyngeal Carcinoma by Using the Computed Tomography-Based Radiomics," *Contrast Media & Molecular Imaging*, vol. 2022, Article ID 3417480, 8 pages, 2022.

Hindawi
Contrast Media & Molecular Imaging
Volume 2022, Article ID 3417480, 8 pages
https://doi.org/10.1155/2022/3417480

Research Article

Prediction of Changes in Tumor Regression during Radiotherapy for Nasopharyngeal Carcinoma by Using the Computed Tomography-Based Radiomics

Yu Yang, Jiayang Wu, Wenfeng Mai, and Hengguo Li

Medical Imaging Center, The First Affliated Hospital of Jinan University, Guangzhou 510630, China

Correspondence should be addressed to Hengguo Li; 17020204210006@hainanu.edu.cn

Received 30 June 2022; Revised 20 August 2022; Accepted 8 September 2022; Published 23 September 2022

Academic Editor: Sorayouth Chumnanvej

This work aimed to explore the application value of computed tomography (CT)-based radiomics in predicting changes in tumor regression during radiotherapy for nasopharyngeal carcinoma. In this work, 144 patients with nasopharyngeal carcinoma who underwent concurrent chemoradiotherapy (CCRT) in our hospital from January 2015 to December 2021 were selected. The patients were divided into a radiosensitive group (79 cases) and an insensitive group (65 cases) according to the tumor volume shrinkage during radiotherapy. The 3D Slicer 4.10.2 software was used to delineate the tumor region of interest (ROI), and a total of 1223 radiomics features were extracted using the radiomics module under the software. After between-group and within-group consistency tests, one-way ANOVA, and LASSO dimensionality reduction, three omics features were finally selected for the establishment of predictive models. At the same time, the age, gender, tumor T stage and N stage, hemoglobin, and albumin of the patients were collected to establish a clinical prediction model. The results showed that compared with logistic regression, decision tree, random forest, and AdaBoost models, the SVM model based on CT radiomics features had the best performance in predicting tumor regression changes during tumor radiotherapy (training group area under the receiver operating characteristic curve (AUC): 0.840 (95% confidence interval (CI): 0.764–0.916); validation group: AUC: 0.810 (95% CI: 0.676–0.944)). Compared with the supported vector machine (SVM) prediction model based on clinical features, the SVM model based on radiomics features had better performance in predicting the change of retraction during tumor radiotherapy (training group: omics feature SVM model AUC: 0.84, clinical feature SVM model: 0.78; validation group: omics feature SVM model AUC: 0.8, clinical feature SVM model: 0.58, $P = 0.044$). Based on the radiomics characteristics and clinical characteristics of patients, a nomo prediction map was established, and the calibration curve shows good consistency, which can be visualized to assist clinical judgment. In this work, the prediction model composed of CT-based radiomic features combined with clinical features can accurately predict withdrawal changes during tumor radiotherapy, ensuring the accuracy of treatment planning, and minimizing the number of CT scans during radiotherapy.

1. Background

Intensity-modulated radiation therapy (IMRT) [1] is the main method for the treatment of nasopharyngeal carcinoma. Compared with two-dimensional radiotherapy, it can further improve the local tumor control rate and improve the survival of patients [2]. However, IMRT also has its downsides. During treatment, due to factors such as tumor tissue shrinkage, normal tissue changes, and patient nutritional status changes, the steep treatment dose distribution can lead to deviations between the tumor and the irradiation target interval, resulting in insufficient irradiation dose at the edge of the tumor or normal tissue falling into high dose area [3]. To solve this problem, adaptive radiation therapy (ART) came into being [4]. Studies have shown that adaptive radiotherapy is of great value in ensuring the target dose, reducing the dose to the parotid gland and other organs, and protecting normal tissues [5]. However, there are also many problems in the application of ART technology. For example, the treatment process is time-consuming, the patient

cannot tolerate it, it occupies a lot of resources, and the patient receives too much radiation [6].

Further research found that (1) during the implementation of ART technology, the degree of changes in tumor regression is closely related to the dose range of the irradiation target area and the irradiation dose of adjacent normal tissues and organs [7]. (2) The degree of tumor regression varies among patients during treatment, and some patients have no significant changes in tumor volume during the pre-course and mid-course treatment (possibly due to radiation resistance) [8]. In view of this, some scholars believe that these patients may not benefit from ART, and may not need ART at least in the first and middle course of treatment. Therefore, it is of great significance to explore a new technique or method to assist in the assessment of the degree of regression changes during radiotherapy in patients with nasopharyngeal carcinoma before radiotherapy, so as to help the clinical improvement of treatment planning. (3) Radiomics has shown its important value in the diagnosis and differential diagnosis of nasopharyngeal carcinoma, short-term and long-term efficacy evaluation, survival, and prognosis evaluation [9]. However, there are few reports on predicting changes in tumor regression during radiotherapy.

The focuses of this work are summarized as follows: (1) It retrospectively collected a batch of patients with nasopharyngeal carcinoma radiotherapy and gave localization computed tomography (CT) scans at the beginning of radiotherapy and at about 20 points during radiotherapy. (2) It compared the CT images before and after to judge the changes in tumor regression during radiotherapy. The patients were divided into a response group and a nonresponse group according to the judgment criteria established in the literature. (3) It extracted the CT omics characteristics of the tumor before radiotherapy, analyzed them statistically, and modeled them.

2. Materials and Methods

2.1. Basic Data of Patients. This experiment was approved by the hospital ethics committee, exempting patients from informed consent. A total of 262 patients with nasopharyngeal carcinoma who underwent CCRT in our hospital from January 2015 to December 2020 were collected. All patients were diagnosed by nasopharyngeal biopsy, and the pathological types were undifferentiated nonkeratinizing carcinoma. Inclusion criteria were set as follows: (1) The age of the patients was more than 18 years old; (2) the Karnofsky score [10] of the physical condition before treatment was ≥ 70 points; (3) the blood routine, liver and kidney function, and other indicators were normal before treatment, and there was no contraindication of radiotherapy and chemotherapy; (4) the informed consent for radiotherapy/chemotherapy was signed before treatment; and (5) the radiotherapy/chemotherapy treatment was successfully completed. The exclusion criteria were defined as follows: (1) the patients had a history of head and neck radiotherapy and surgery; (2) the patients suffered from cardiovascular and cerebrovascular diseases, diabetes, and other basic diseases, and could not receive treatment; (3) the patients failed to successfully complete radiotherapy and chemotherapy; and (4) The collected data were incomplete.

Among all patients, 175 patients had complete CT scan images before and during radiation therapy (16th to 20th fraction of the course), and 87 patients had only CT images before radiation therapy but lacked CT images during radiation therapy, who were excluded. In addition, 18 patients were excluded due to image artifacts (including 11 denture artifacts and 7 motion artifacts) and 13 patients were excluded due to incomplete clinical data. Finally, 144 patients were included in this work. Figure 1 illustrated the specific flow chart of case collection.

The clinical data of the patients were collected, including name, gender, age, tumor T stage, clinical tumor stage, albumin, and hemoglobin counts before treatment. Among the144 patients included in this work, there were 106 males and 39 females, and they were 18–79 years old, with an average age of 52 years. According to the 2017 Chinese nasopharyngeal carcinoma staging method, there were 18 cases of T1 stage, 72 cases of T2 stage, 30 cases of T3 stage, and 24 cases of T4 stage. There were 85 cases of clinical stage II, 33 cases of stage III, and 26 cases of stage IV. The albumin was 30.2–56.3 g/l, with an average value of 43.7 g/l; and the hemoglobin was 91–172 g/l, with an average value of 136 g/l before treatment.

The CT images before and after the treatment of each patient were segmented and the volume was extracted. According to the segmented whole tumor region of interest (ROI), the tumor volume was extracted under the three-dimensional Slice software model module. The tumor volume changes before and during radiotherapy were compared for each patient, and the tumor shrinkage ratio was calculated. The tumor volume reduction ratio ranged from 12% to 87%, with an average tumor reduction of 54% and a median tumor reduction of 51%. Taking the median of 51% as the standard, the patients were divided into 2 groups as follows: 79 cases in the sensitive group and 65 cases in the insensitive group.

2.2. Treatment Plan. All patients were treated with simultaneous IMRT + chemotherapy treatment mode. Based on the physical condition and response after chemotherapy of patients, 1–2 cycles of induction chemotherapy should be given to patients with clinical stages III and IV before receiving concurrent radiotherapy/chemotherapy. After radiotherapy, 3–4 cycles of adjuvant chemotherapy were given, and the chemotherapy regimens were all platinum ± paclitaxel-containing regimens. Radiation therapy was performed using 7-field intensity-modulated radiation therapy mode, 6 MV photon irradiation, PGTV: 70–74 Gy, PGTVnd: 68–72 Gy, CTV1: 60–64 Gy, and CTV2: 50–54 Gy. It should be repeated for 32–35 times of irradiation, irradiated once a day, 5 times a week, continuous irradiation.

2.3. CT Scanning. Enhanced helical CT scans were performed before treatment and on the 16th to 20th times during the radiotherapy. The TOSHIBA Aquilion 16 scanner

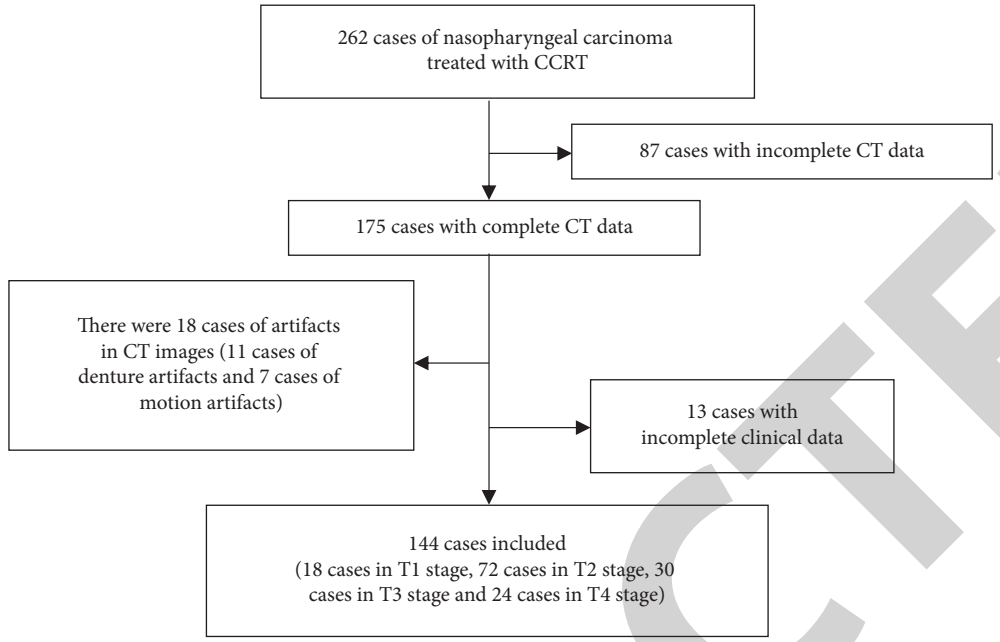

Figure 1: Flow chart of case collection.

produced by Toshiba Corporation of Japan was used [11]. The scanning range included the Sella to the plane of the lower border of the bilateral clavicle heads. X-ray tube voltage was 125 Kv, and tube current was 250 mA. The layer thickness and interval of the two scans were the same, both of which were 3 mm. Consecutive cross-sectional images were acquired while scanning. The enhanced contrast agent was the iodine contrast agent (iodine 300), which was injected with a high-pressure syringe at an injection rate of 3 mL/s, and the scan was started 30 seconds after injection [12].

2.4. Image Preprocessing and ROI Segmentation. Enhanced CT images (DICOM format) of patients were acquired before and after radiotherapy in preparation for ROI segmentation [13]. The first was to preprocess the CT image. (1) Resampling: the image was processed in the radiomics working directory (resampling voxel size: 1, 1, 1). (2) Grayscale normalization: before feature extraction, the Bin width was adopted to normalize the discrete grayscale values of the image. (3) Standardization: the image data matrix was normalized by Z-score. The nasopharyngeal carcinoma lesions in CT images were segmented by the open-source 3D Slicer4.10.2 (http://www.slicer.org) segmentation software. Manual segmentation based on the working directory of the segment editor, and sketching layer by layer. It should note that nonlesion images, such as adjacent skull base bone, tumor necrosis area, and enhanced thickened vascular shadows, should be avoided when delineating, and finally the full tumor ROI of the lesion should be determined.

2.5. Radiomics Feature Extraction, Consistency Check, Screening, and Model Construction. The open-source 3D Slicer4.10.2 (http://www.slicer.org) software was used to extract CT radiomics group features. After the whole tumor ROI was determined, the core step of radiomics was to extract high-throughput features to quantitatively analyze the substantial properties of the ROI. The extracted features can be roughly divided into the following four categories: (1) first-order statistical features; (2) shape and size features; (3) texture features, including gray level dependence matrix (GLDM), gray level size zone matrix (GLSZM), gray level co-occurrence matrix (GLCM), gray level run length matrix (GLRLM), and neighboring gray tone difference matrIX (NGTDM); and (4) wavelet features.

20 randomly selected cases were delineated by two head and neck physicians with more than ten years of work experience within one month, and the intragroup and intergroup consistency tests were carried out. The radiomics group characteristics with ICC <0.75 were given culls.

Radiomics feature screening and model construction process were described as follows: (1) The Least absolute shrinkage and selection operator (Lasso) algorithm was employed to filter features, determine the number of features according to the convergence graph and Log(λ) graph, and establish a function. (2) After the function was established, the radiomics score of each case was calculated. The prediction model was constructed based on a support vector machine (SVM), and the model parameters were optimized through 10-fold cross-validation to improve the performance of the optimized model.

2.6. Establishment and Validation of Radiomics Model. After the data were divided into the training set and the validation set, the AUC, sensitivity, specificity, positive predictive value (PPV), negative predictive value (NPV), and accuracy of the two groups were compared and analyzed, and the predictive effect of CT-based radiomics

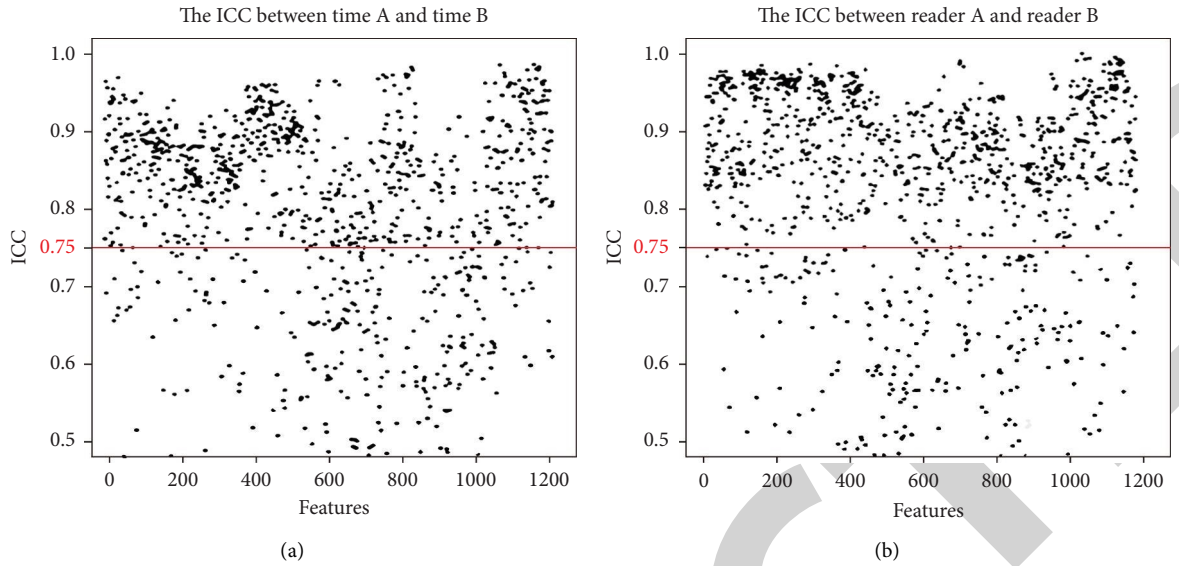

Figure 2: The intragroup and intergroup ICC results of image feature extraction. Note: The ordinate represented the ICC value, the abscissa represented the radiomics group characteristics, and above the horizontal red line were the radiomics features with ICC greater than 0.75.

characteristics in the degree of tumor regression in radiotherapy patients was used [14].

2.7. Combination of Clinical-Radiomics Features and Construction of a Nomogram to Predict Changes in Tumor Regression during Radiotherapy. Univariate analysis was performed on the collected clinical and CT image features, and the variables with significant differences were combined with radiomics to establish a multivariate regression model. The above indicators were evaluated and compared with the clinical data and the prediction effect of the radiomics group, and finally, a clinical-radiomics group prediction nomogram was created [15]. Finally, a decision curve and a calibration curve were drawn to evaluate its predictive performance and calibration.

2.8. Statistical Analysis. SPSS software (version 21.0, SPSS Inc., Chicago, IL, USA) was used. The measurement data were represented by the mean ± standard deviation ($\bar{X} \pm SD$) and the count data were represented by count and percentage, and they were compared using independent samples *t*-test, rank-sum test, and chi-square test, respectively. Logistic regression analysis was used for multivariate analysis, and $P < 0.05$ indicated the difference was statistically significant. If the ICC or Kapp value was greater than 0.75, the consistency was considered to be good.

3. Results

3.1. Radiomics Features Consistency Test, Feature Screening Results, and Function Establishment. 20 cases were randomly selected. R language software (R x64 3.6.0, Rstudio) was used to perform ICC tests within (A) and between (B) groups, and the test level was set at 0.75, as shown in Figure 2. After testing, a total of 559 features < 0.75 were excluded, and 664 features were greater than 0.75.

The above-mentioned features with an ICC between groups greater than 0.75 were used in different sequences to reduce dimensionality using LASSO to remove redundant features. The results showed that a total of 3 significantly different radiomics characteristics were screened, as shown in Figure 3 and Table 1.

3.2. Comparison on Prediction of Radiomics Model Based on SVM. Rstudio randomly divided all the patients into a training set and a validation set, the final training set was 100 cases, and the validation set was 44 cases. As shown in Figures 4 and 5, compared with the SVM prediction model based on clinical features, the SVM model based on radiomics features had better performance in predicting the change of regression during tumor radiotherapy (training group: omics feature SVM model AUC: 0.84, clinical feature SVM model: 0.78; validation group: omics feature SVM model AUC: 0.8, clinical feature SVM model: 0.58, $P = 0.044$).

3.3. Nomogram for Combined Clinical-CT Radiomics Model Predictions. The patient's age, gender, tumor T stage and N stage, hemoglobin, albumin, etc. were collected to establish a clinical prediction model. The results were shown in Figure 6. At the same time, a nomogram prediction map was established based on the radiomics characteristics and clinical characteristics of the patients, and the calibration curve showed good consistency, as shown in Figure 7.

3.4. Validation of Nomograms Related to Clinical-Radiomics. Compared with logistic regression, decision tree, random forest, and AdaBoost models, the SVM model based on CT radiomics features had the best performance in predicting

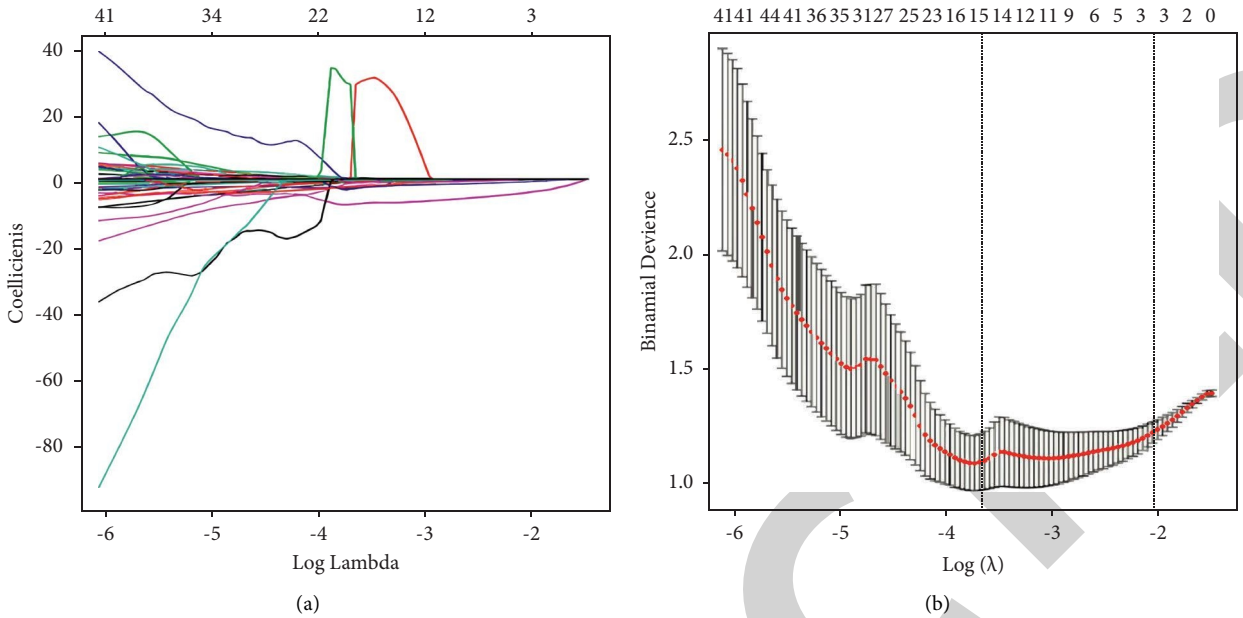

Figure 3: Features with an image ICC greater than 0.75, the results of feature screening using the LASSO method. (a) shows the centralized convergence diagram of the feature, the abscissa was the Lambda value, and the ordinate was the feature coefficient; (b) shows the model selection and result of feature selection, the abscissa was the Lambda value, and the ordinate was the variance. According to the principle of the most concise model, 3 features were screened.)

Table 1: Feature names and correlation coefficients selected for modeling after LASSO.

Feature name	Radiomics feature or constant	Coefficient
X12	Original-shape-Minor Axis Length	−0.7579559
X56	Log-sigma-0–5-mm-3d first-order Median	−0.1419084
X487	Wavelet-LHL-GLDM-Dependence Nonuniformity Normalized	−4.2839436

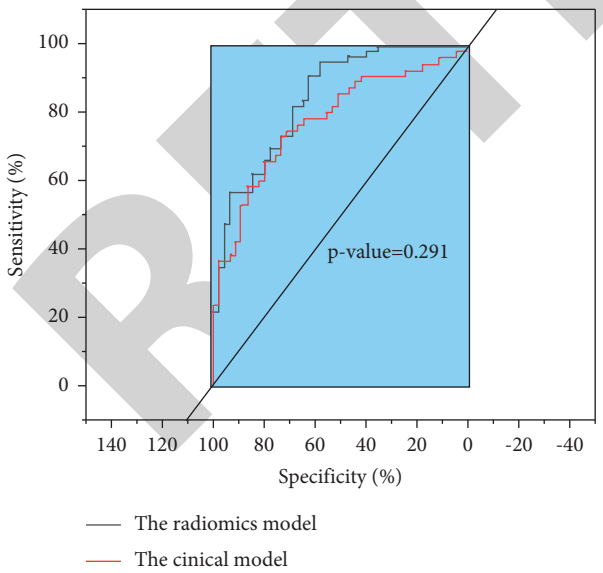

Figure 4: Comparison of ROC of the training group and clinical group.

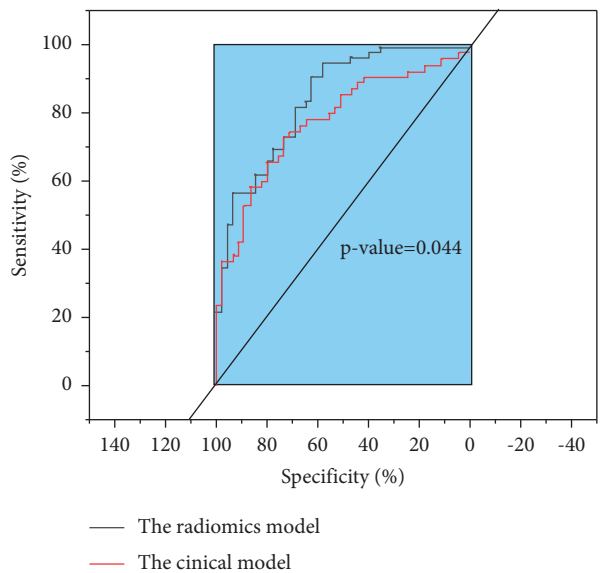

Figure 5: Comparison of ROC of the validation group and clinical group.

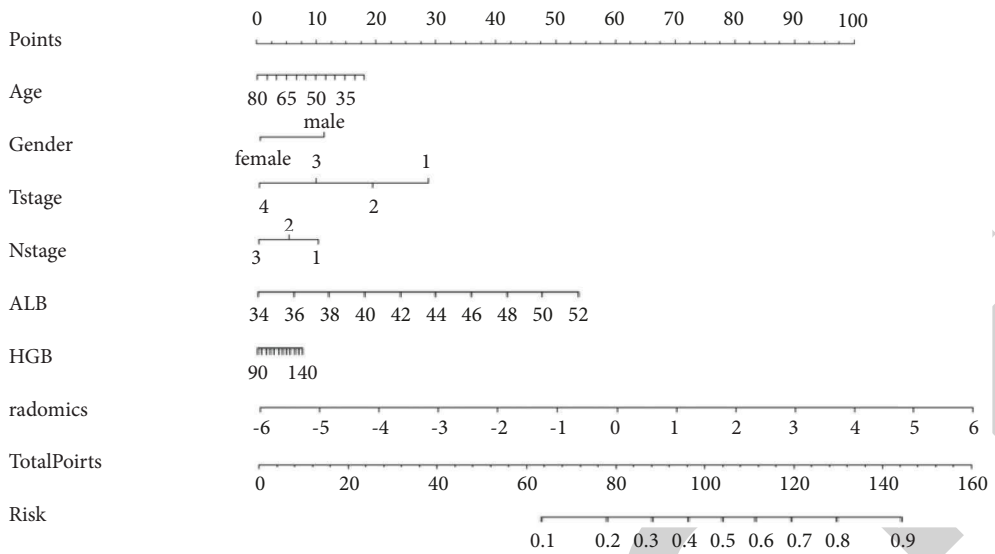

Figure 6: Nomogram constructed from clinical and CT radiomics features.

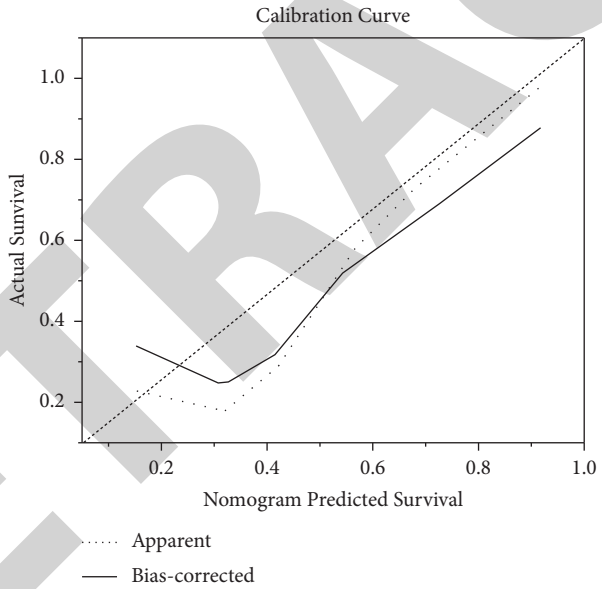

Figure 7: Calibration curve constructed based on the nomogram.

Table 2: Statistics on the diagnostic efficacy of different models in the training and validation groups.

Model	Group	Sensitivity	Specificity	PPV	NPV	Accuracy	*F*1
Logistic	Training	0.800	0.622	0.721	0.718	0.720	0.759
	Test	0.792	0.350	0.594	0.583	0.591	0.679
Decision tree	Training	0.909	0.711	0.794	0.865	0.820	0.847
	Test	0.917	0.400	0.647	0.800	0.682	0.759
Random forest	Training	1.000	1.000	1.000	1.000	1.000	1.000
	Test	0.875	0.550	0.700	0.786	0.727	0.778
SVM	Training	0.909	0.622	0.746	0.848	0.780	0.820
	Test	0.875	0.250	0.583	0.625	0.591	0.700
AdaBoost	Training	0.782	0.867	0.878	0.765	0.820	0.827
	Test	0.792	0.450	0.633	0.643	0.636	0.704

tumor regression changes during tumor radiotherapy (training group AUC: 0.840 (95% CI: 0.764–0.916); validation group: AUC: 0.810 (95% CI: 0.676–0.944)), as shown in Table 2.

4. Discussion

Nasopharyngeal carcinoma patients are sensitive to radiation. During radiotherapy, the relative position of anatomical structures changes due to the retraction of the primary tumor and metastatic lymph nodes and the loss of body weight, so that the actual dose obtained deviates from the initially prescribed dose [16]. In this work, CT images were used to delineate and compare the tumor lesions of radiotherapy-sensitive patients and radiotherapy-insensitive patients with nasopharyngeal carcinoma, and the SVM was used to build a model and conduct training analysis. The results showed that compared with the SVM prediction model constructed based on clinical features, the SVM model constructed based on radiomics features had better performance in predicting the change of retraction during tumor radiotherapy. In addition, compared with logistic regression, decision tree, random forest, and AdaBoost models, the SVM model based on CT radiomics features had the best performance in predicting tumor regression changes during tumor radiotherapy. Previous studies have also found that hat the general linear classification method achieved poor results, which may be related to individual differences and differences in different microscopic manifestations of tumors [17]. Based on the radiomics and clinical characteristics of patients, a nomogram prediction map is established, and the calibration curve shows good consistency, which can be visualized to assist clinical judgment.

In conclusion, CT radiomics features can objectively reflect the dynamic changes of tumor heterogeneity in nasopharyngeal carcinoma and quantify the difference between tumor and normal tissue, so it can be used to identify tumor tissue, excluding the effect of enhancer on CT images of each phase, and reduce delineation error [18]. The results of Peng et al. showed that the radiomics model outperformed the EBV DNA model (0.754 vs. 0.675 for the training set and 0.722 vs. 0.671 for the test set) [19]. The research results of Yan et al. showed that the nomogram constructed based on CT (C index, 0.873, 95% confidence interval (CI): 0.803–0.943) was superior to the clinical nomogram in prediction (C index, 0.729, 95% CI: 0.620–0.838) and tumor node metastasis (TNM) staging system (C index, 0.689, 95% CI: 0.592–0.787) [20]. This is consistent with the results of this work.

5. Conclusions

The results of this work showed that a predictive model composed of CT-based radiomics combined with clinical features can accurately assess the changes in tumor regression during radiotherapy and ensure the accuracy of treatment plans, and using this prediction method can help reduce the number of CT scans during radiation therapy in patients. However, the sample size included was small, and individual differences may have a certain impact on the results, which needed to be further confirmed in future research. In conclusion, CT radiomics features can be used to visualize and assist in the assessment of tumor status in patients with nasopharyngeal carcinoma undergoing radiotherapy, which had clinical application value.

Data Availability

The data used to support the findings of this study are available from the corresponding author upon request.

Conflicts of Interest

The authors declare that they have no conflicts of interest.

References

[1] S. A. Yeh, T. Z. Hwang, C. C. Wang, C. C. Yang, and T. F. Lee, "Outcomes of patients with nasopharyngeal carcinoma treated with intensity-modulated radiotherapy," *Journal of Radiation Research*, vol. 62, no. 3, pp. 438–447, 2021.

[2] H. Minatogawa, K. Yasuda, Y. Dekura, S. Takao, and H. Shirato, "Potential benefits of adaptive intensity-modulated proton therapy in nasopharyngeal carcinomas," *Journal of Applied Clinical Medical Physics*, vol. 22, no. 1, pp. 174–183, 2021.

[3] A. W. M. Lee, W. T. Ng, J. Y. W. Chan et al., "Management of locally recurrent nasopharyngeal carcinoma," *Cancer Treatment Reviews*, vol. 79, Article ID 101890, 2019.

[4] X. S. Sun, X. Y. Li, Q. Y. Chen, L. Q. Tang, and H. Q. Mai, "Future of radiotherapy in nasopharyngeal carcinoma," *British Journal of Radiology*, vol. 92, no. 1102, Article ID 20190209, 2019.

[5] S. A. Arslan, "Clinical outcomes of nasopharyngeal carcinoma patients treated with adaptive helical tomotherapy, A 5-year experience," *Nigerian Journal of Clinical Practice*, vol. 23, no. 12, pp. 1683–1689, 2020.

[6] D. Mark, P. Gilbo, R. Meshrekey, and M. Ghaly, "Local radiation therapy for palliation in patients with multiple myeloma of the spine," *Frontiers in Oncology*, vol. 9, p. 601, 2019.

[7] H. Piperdi, D. Portal, S. S. Neibart, N. J. Yue, and M. Reyhan, "Adaptive radiation therapy in the treatment of lung cancer: an overview of the current state of the field," *Frontiers in Oncology*, vol. 11, Article ID 770382, 2021.

[8] Z. Végváry, B. Darázs, V. Paczona et al., "Adaptive radiotherapy for glioblastoma multiforme - the impact on disease outcome," *Anticancer Research*, vol. 40, no. 8, pp. 4237–4244, 2020.

[9] A. Shayah, L. Wickstone, E. Kershaw, and F. Agada, "The role of cross-sectional imaging in suspected nasopharyngeal carcinoma," *Annals of the Royal College of Surgeons of England*, vol. 101, no. 5, pp. 325–327, 2019.

[10] A. Mehta, E. Chai, K. Berglund, and L. P. Gelfman, "Using admission karnofsky performance status as a guide for palliative care discharge needs," *Journal of Palliative Medicine*, vol. 24, no. 6, pp. 910–913, 2021.

[11] Y. Ren, H. Qiu, Y. Yuan et al., "Evaluation of 7th edition of AJCC staging system for nasopharyngeal carcinoma," *Journal of Cancer*, vol. 8, no. 9, pp. 1665–1672, 2017.

[12] J. Yao, P. Yang, L. Zhao, Z. Xu, and C. Chen, "Radiomics features of ascending and descending nasopharyngeal

carcinoma," *Zhong Nan Da Xue Xue Bao Yi Xue Ban*, vol. 45, no. 7, pp. 819–826, 2020.

[13] C. Hu, D. Zheng, X. Cao, P. Pang, and Y. Chen, "Application value of magnetic resonance radiomics and clinical nomograms in evaluating the sensitivity of neoadjuvant chemotherapy for nasopharyngeal carcinoma," *Frontiers in Oncology*, vol. 11, Article ID 740776, 2021.

[14] S. J. Elberts, R. Bateman, A. Koutsoubis, and J. M. Fields, "The impact of COVID-19 on the sensitivity of D-dimer for pulmonary embolism," *Academic Emergency Medicine*, vol. 28, no. 10, pp. 1142–1149, 2021.

[15] Q. Cui, L. Sun, Y. Zhang et al., "Value of breast MRI omics features and clinical characteristics in Breast Imaging Reporting and Data System (BI-RADS) category 4 breast lesions: an analysis of radiomics-based diagnosis," *Annals of Translational Medicine*, vol. 9, no. 22, p. 1677, 2021.

[16] R. You, Y. P. Liu, P. Y. Huang, X. Zou, and M. Y. Chen, "Efficacy and safety of locoregional radiotherapy with chemotherapy vs chemotherapy alone in de novo metastatic nasopharyngeal carcinoma: a multicenter phase 3 randomized clinical trial," *JAMA Oncology*, vol. 6, no. 9, pp. 1345–1352, 2020.

[17] R. Aswarin, M. Yusuf, and M. S. Wiyadi, "Association of protein expression p53 mutants with regional lymph gland status on type III carcinoma nasofaring patients," *Indian Journal of Otolaryngology and Head & Neck Surgery*, vol. 70, no. 3, pp. 405–409, 2018.

[18] C. Xie and V. Vardhanabhuti, "PET/CT: nasopharyngeal cancers," *PET Clinics*, vol. 17, no. 2, pp. 285–296, 2022.

[19] H. Peng, D. Dong, M. J. Fang et al., "Prognostic value of deep learning PET/CT-Based radiomics: potential role for future individual induction chemotherapy in advanced nasopharyngeal carcinoma," *Clinical Cancer Research*, vol. 25, no. 14, pp. 4271–4279, 2019.

[20] C. Yan, D. S. Shen, X. B. Chen et al., "CT-based radiomics nomogram for prediction of progression-free survival in locoregionally advanced nasopharyngeal carcinoma," *Cancer Management and Research*, vol. 13, pp. 6911–6923, 2021.